Flow Boiling of R245fa in a Microgap with Integrated Staggered Pin Fins

Pouya Asrar, Xuchen Zhang, Casey D. Woodrum, Craig E. Green, Peter A. Kottke, Thomas E. Sarvey, Suresh Sitaraman, Andrei Fedorov, Muhannad Bakir, and Yogendra K. Joshi*,§
*George W. Woodruff School of Mechanical Engineering, Georgia Institute of Technology, Atlanta, GA 30332, United States
§Corresponding author. Fax: +1 404-894-8496 Email: yogendra.joshi@me.gatech.edu

ABSTRACT

We present an experimental study of two phase flow of refrigerant R245fa in a pin fin enhanced microgap for a range of heat fluxes between 151 W/cm^2 to 326 W/cm^2. The gap has a base surface area of 1cm x 1cm and height of 200 µm. An array of hydrofoil shaped pin fins covers from bottom to top of the microgap. The pin fins have chord length, longitudinal pitch, and transversal pitch of 75µm, 450µm and 225µm, respectively. On the back side of the chip, four platinum heaters are fabricated and electrically powered in series to enable two phase flow in the microgap, which was part of a pumped flow loop. Heater and surface temperature data were obtained versus heat flux dissipated. Flow visualization was performed using a high speed camera in the heat flux range from 151 W/cm^2 to 326 W/cm^2. The amount of heat loss across the test section is also provided.

KEY WORDS: microgap flow boiling heat transfer, microelectronic cooling, pin fin

NOMENCLATURE

C	Hydrofoil Pin Fin Chamber Length, µm
D	Hydrofoil Pin Fin Height, µm
D_p	Redistribution line pin fin diameter, µm
G	mass flux, kg/(m^{2}s)
H	microgap height, µm
k	thermal conductivity, W/(m K)
L	microgap length, cm
P_L	Longitudinal Pitch, µm
P_T	Longitudinal Pitch, µm
q''	heat flux, W/cm^2
T_H	microgap bottom (surface) temperature, ℃
T_{surf}	microgap bottom (surface) temperature, ℃
W	microgap width, cm
x	exit vapor mass quality

INTRODUCTION

As seen in Table 1, dissipation of heat fluxes as high as hundreds of W/cm^2 using flow boiling has been investigated previously[1-5]. Dielectric liquids have been investigated, as they allow direct contact with active electronics. However, due to the significantly lower thermal conductivity of these liquids than water, two-phase heat transfer is typically utilized to achieve higher heat transfer coefficients. Kosar et al.[6] investigated the forced convection flow boiling of refrigerant R-123 over the range of heat flux between 3.5 to 65.5 W/cm^2. The microchannel device was 1.8 mm wide and 1 cm long with the gap height of 243µm. The gap was populated with circular pin fins with longitudinal and transverse pitch of 150 µm. They reported average surface temperature for a range of volumetric flow rate between 3.429-8.047 mL/min. Boiling visualizations were performed for mass fluxes of 351, 752, and 887 kg/m^2. Law et al.[7] considered copper microchannels with two different surface enhancements: straight and oblique fins with dielectric fluid FC-72 as the working fluid. The results were obtained at mass fluxes of 175 kg/m^{2}s and 370 kg/m^{2}s, and heat fluxes ranging from 14 W/cm^2 to 42 W/cm^2. It was concluded that oblique-finned channel showed a significant decrease in temperature and pressure fluctuations in the system under different running conditions.

Lim et al.[8] investigated two phase flow of water in a microchannel with the hydraulic diameter of 500 µm. The upper surface of a copper plate was machined to create the microchannel. Heat was supplied using a film heater attached to the bottom of the copper plate. Mass fluxes of 200, 400, and 600 kg/m^{2}s were studied, and dissipated heat fluxes between 10-40 W/cm^2.

Qu et al.[9] presented results for flow boiling of deionized water in microchannels with 231×713 µm cross section for mass fluxes from 135 to 402 kg/m^{2}s. The boiling curves were obtained for four stream-wise locations. For inlet temperature of 60 ℃, a maximum heat flux of 130 W/cm^2 was demonstrated. The heat transfer coefficient was found to decrease with increasing quality in the microchannel.

Krishnamurthuy et al.[10] considered flow boiling of water in a microchannel equipped with circular staggered pin fins. The experiments were implemented for the mass fluxes in the range of 346 kg/m^{2}s to 794 kg/m^{2}s. The microgap was 10 mm long, 1.8 mm wide, with 250 µm height.

Qu et al.[11] measured the maximum heat flux dissipated in a microgap for water as working fluid at two different fluid inlet temperature conditions: 30 ℃ and 60 ℃.[11] The critical heat fluxes (CHF) at inlet temperature of 30 ℃ and 60 ℃ were reported as 184.4 W/cm^2 and 184.5 W/cm^2, respectively for mass flux of 228 kg/m^{2}s.

Lee et al.[12] investigated the two-phase flow of R134a[12]. Two evaporators were used in the setup which were two microchannel heat exchangers arranged in series. Each of heat exchangers had 1mm^2 cross sectional area and were 152.4 mm and 609.6 mm long. The mass flux and heat flux ranged between 152.90-530.72 kg/m^{2}s and 0.8-4.8 W/cm^2, respectively. The nucleate boiling and slug flow regimes were more dominant at low qualities. Increasing the quality revealed annular flow as well as convective boiling regimes.

The current research is focused on flow boiling of refrigerant R245fa in a microgap 1 cm × 1 cm × 200 µm. It is

noted that the studies listed in Table 1 have focused on microchannels. The device studied has a 1 cm × 1 cm footprint area of staggered hydrofoil pin fins, with the hydraulic diameter of 75µm. Prior to the array of hydrofoil pin fins, four columns of pin fins are densely arranged to evenly distribute the flow in the microchannel. A glass cover is anodically bonded to the silicon microgap, also allowing flow visualization.

Table 1: Current Research vs. Prior Literature

Research Group	W (mm)	L (mm)	H (µm)	Max. Heat Flux (W/cm²)	Max. Mass Flux (kg/cm²s)
Kosar et al.[6]	1.8	10	243	65.5	887
Law et al.[7]	0.3	25	1185	42	370
Lim et al.[8]	0.5	60	500	40	600
Qu et al.[9]	0.2	44.8	713	130	402
Krishnamurthuy et al.[10]	1.8	10	243	350	794
Qu et al.[11]	0.2	44.8	821	184.5	228
Current Research	10	10	200	326	1610

EXPERIMENTAL SETUP AND PROCEDURES

Figure 1 shows the schematic of the experimental setup. The air inside the loop is fully evacuated using a vacuum pump (VN-200N, JB Industries Inc.). In order to charge the system with R245fa, the source tank is heated up to a temperature higher than ambient temperature. After charging the reservoir with enough refrigerant, the reservoir is heated up to few ^{o}C higher than ambient temperature in order to make sure that the pressure inside the reservoir is enough to have the flow always going towards the syringes. The continuous flow is insured by having one of the pumps pushing, and the other one pulling instantly. Once the pumps are fully charged, the refrigerant is pushed by one of the syringe pumps towards the pre-cooler in order to become all in liquid phase. After leaving the pre-cooler, the working fluid volumetric flow rate is measured by a microturbine flow meter (S-114, Mcmillan Co.). R245fa then becomes contaminant free by passing through a 0.5 **µm** filter (SS-4F-05, Swagelok Co.). The 0.5 **µm** in-line filter prevents contaminants from entering the device. The flow loop is equipped with a back wash circuit to be able to run the fluid through the chip in both directions for the purpose of cleaning it before running the actual test. The fluid comes back to the reservoir after cooling down in the heat exchanger that is located right after the test section. The refrigerant is pushed through the test device at a certain flow rate and becomes hot. It then enters the heat exchanger (LL510G14, Lytron Co.) to become cool enough before coming back to the reservoir.

The system is run for a few hours and all properties such as pressures, temperatures, and flow rate are recorded by the data acquisition unit to guarantee steady state before running the thermal test. The systems properties (temperature and pressure) need to stay at a certain constant value in each cycle of pushing in order to guarantee the steady state condition of running the experiment. Once steady state is reached, the heaters are powered gradually starting from heat flux of ~1 W/cm^2. The voltage and current applied to the heaters are recorded for heat flux calculations.

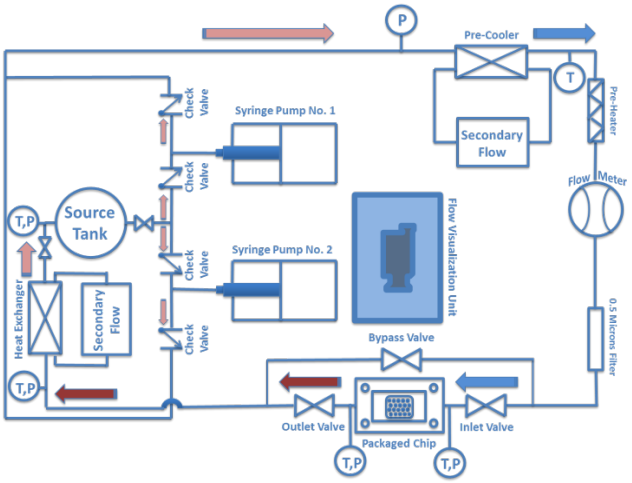

Figure 1: Schematic of the Flow Loop

The flow boiling inside the microgap is visualized with a high speed camera (Phantom V211, VISION Research Co.), at 2,229 frames per second. All measured data for temperature, pressure, voltage and the current are recorded for each heat flux value.

Figure 2 illustrates the schematic of the test device. The fabrication process is provided in the next section. The chip is sealed between a printed circuit board (PCB) and a package made of peek material. O-rings are used to seal the ports on the device. Using wirebonding process, the electrical connection from the chip to the PCB is done. Using two T-type 1.56 mm diameter thermocouples, temperature data is obtained at the inlet and outlet of the device. The pressures at the inlet and outlet are also recorded using two pressure transducers connected to the pressure measurement ports fabricated on the chip. Staggered hydrofoil pin fins are arranged inside the 1cm^2 microgap. The pin fins are NACA 66-021 hydrofoils also investigated by Kosar et al.[13]. The arrays of flow redistribution pin fins upstream of the hydrofoil pin fins are clearly visible in figure 2. The device dimensions are provided in Table 2.

Table 2: Device Dimensions

Microchannel and Pin Fin Arrays Configuration						
D (µm)	C (µm)	P_L (µm)	P_T (µm)	W (mm)	L (mm)	H (µm)
31.5	150	180	180	10	10	200
Redistribution Pin Fins Configuration						
D_p (µm)		P_L (µm)		P_T (µm)		
90		20		20		

Four platinum heaters dissipate the power through the microchannel. These heaters also serve as resistance temperature detectors (RTDs) and are calibrated in the oven

for the range between 22-125 ℃, displaying a near linear response.

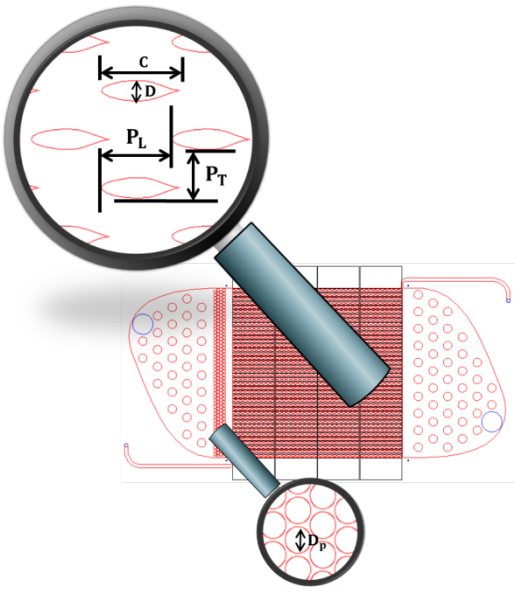

Figure 2: Schematic of the Test Device

Figure 3 shows temperature-resistance curves for all four platinum heaters displaying a linear behavior.

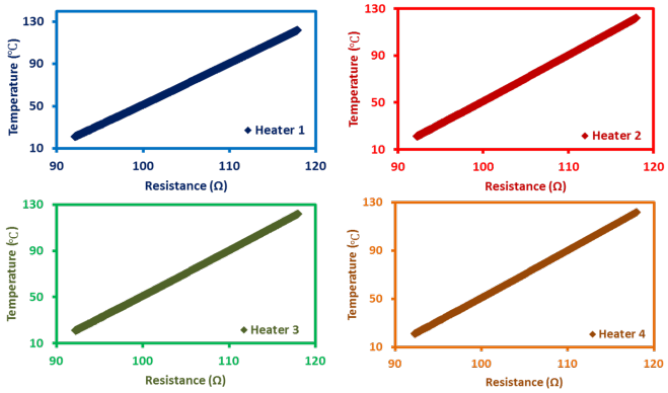

Figure 3: Calibration Curve for the Four Platinum Heaters

The refrigerant enters the heat exchanger after leaving the device to be cooled down before getting back to the reservoir.

FABRICATION PROCESS

The heat sink testbed consists of a 1 cm x 1 cm array of staggered hydrofoil micropin-fins, as shown in figure 4 (left). In addition to fluid inlet and outlet ports, pressure ports are included on either side of the pin-fin arrays in order to accurately measure pressure drop across the gap, while excluding pressure drop due to rapid flow constriction/expansion at the inlet and outlet ports. Four columns of micropin-fins are also introduced upstream of the hydrofoil fins in order to promote a stable and evenly distributed flow. Large mechanical support pins were added near the inlet and outlet for increasing structural strength. Four serpentine platinum heaters/resistance temperature detectors (RTDs) generate heat load and provide temperature measurements in four sections along the flow length (between inlet and outlet).

The process used to fabricate the heat sink testbed is shown in figure 4 (right), starting with a 500 µm thick double side polished wafer. A standard Bosch process was used to create the 200 µm high micropin-fins and manifolds. Next, the cavities formed during etching were sealed using a pyrex cap with anodic bonding at a voltage of 800 V at 350 ℃. The bonded wafer was then flipped over and a 1 µm thick insulating silicon dioxide layer was deposited using chemical vapor deposition (CVD). 200 nm thick Platinum heaters and 500 nm thick gold pads were then deposited on the SiO_2 layer. Another 1 µm thick silicon dioxide passivation layer was deposited on the heaters for protection and thermal isolation. Lastly, inlet, outlet, and the pressure measurement ports were etched using Bosch process from the same side of the wafer.

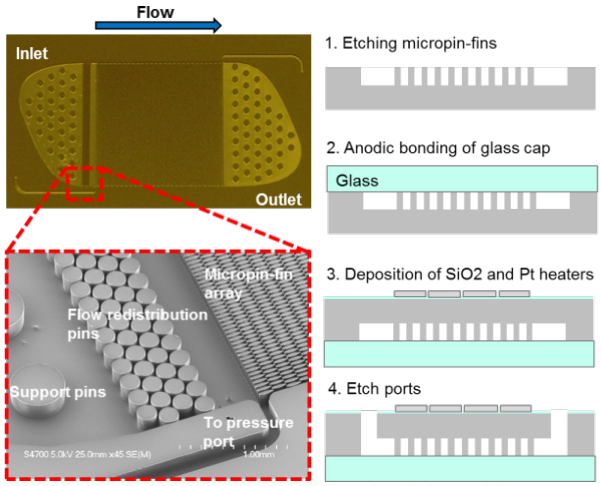

Figure 4: SEM Picture of the Device (left), and the Schematic of the Fabrication Steps (right)

RESULTS AND DISCUSSION

The experiments were done for the inlet temperature of 10 ± 0.5 °C. The flow rate was initially set to 120 mL/min. After reaching steady state condition, a very small amount of power was applied to all four integrated heaters fabricated on the back of the chip. The power was gradually increased until flow boiling was observed. The boiling first started near the outlet pin fin array, and upon increasing the heat flux proceeded towards the inlet of the microgap. Figure 5 demonstrates the visualizations of the flow boiling for a range of heat flux between 150-326 W/cm^2. The majority of the two phase flow was located at the top of the chip close to the outlet. However by increasing the heat flux, the boiling occurred over a larger area inside the microgap. The chip outlet started to dry up partially at 260 W/cm^2 (Figure 5.C). The dry up region expanded and occupied more area in the device as heat flux increased.

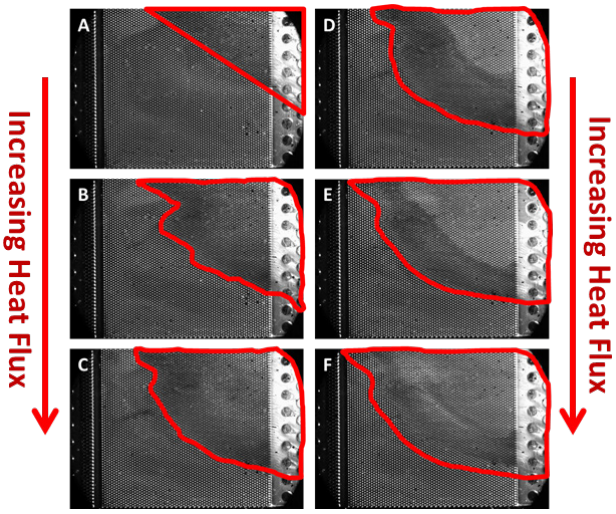

Figure 5: Flow Visualization for a Range of Heat Flux (W/cm^2): A) 150 , B) 210 , C) 260 , D) 264, E) 298, and F) 326 . The red regions indicate flow is either in two phase, or vapor condition.

The maximum temperature of 170 ℃ was recorded at heater 4 and the dissipated power to the chip was 296 W/cm^2. The experiment was stopped at that point and the flow rate was changed from 120 ml/min to 140 mL/min. Figure 8 depicts the temperature distribution of all four heaters versus the heat fluxes that were applied to them. The last data point of the graph is related to the experiment that was done under 140 mL/min of flow rate.

Figure 6 illustrates the schematic interpretations of the visualization set presented in figure 5. As shown in the pictures, for the first few heat flux values the majority of the chip is covered by liquid phase (blue solid region). However, as the power was raised, the two phase region expands more through the microgap. For heat fluxes between 264-326 W/cm^2 a third region is developed close to the outlet of the chip, which is mostly covered by vapor (solid gray region). This region caused the surface temperature to increase significantly, as is shown in figure 9.

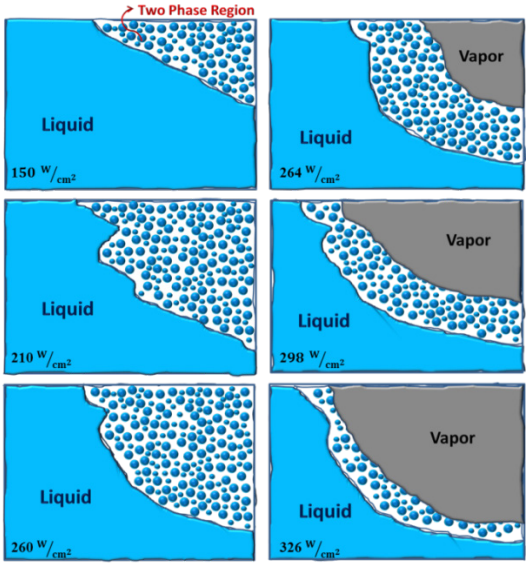

Figure 6: Schematic drawing of flow boiling for different heat flux

The vapor quality in the gap was calculated using Engineering Equation Solver software (EES), based on the pressure and temperature data at the inlet of the microchannel. The maximum quality of 14 % and 6 % was calculated for the flow rates of 120 mL/min and 140 mL/min, respectively. Figure 7 represents the quality data for the heat flux ranging from 184 W/cm^2 to 326 W/cm^2.

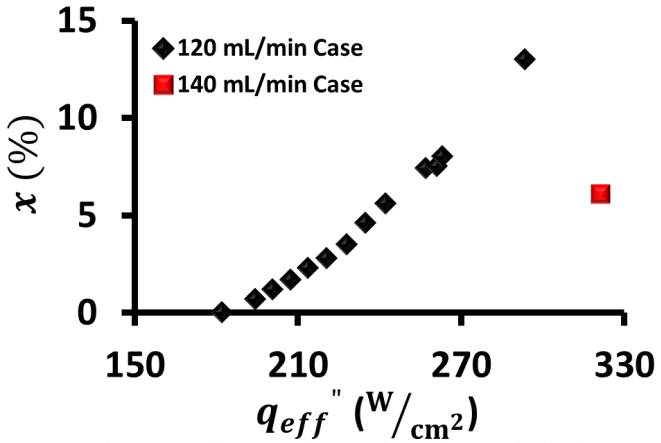

Figure 7: Quality-Heat Flux experimental Data Distribution

As is clear from figure 8, changing the flow rate from 120 mL/min to 140 mL/min enabled lower heater temperatures. Using a 1D heat conduction analysis through the 300 **µm** Si and 2 **µm** SiO_2 layers the surface temperature at the bottom of the microgap was calculated. Figure 9 clearly shows that the surface temperature is lower than the heater temperature because of the convection cooling in the microgap. The results show that the maximum surface temperature at heater 4 location was 160 ℃ at the flow rate of 120 mL/min. For all the experiments in two phase condition, heater 4 showed the highest temperature. In figures 7-9 the heat loss was estimated and applied to the heat flux calculation in order to have a more accurate estimation of the effective power dissipated by the chip.

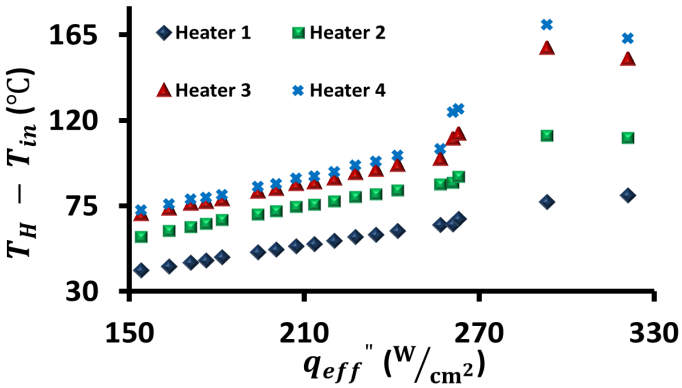

Figure 8: Heater Temperature-Heat Flux Experimental Data

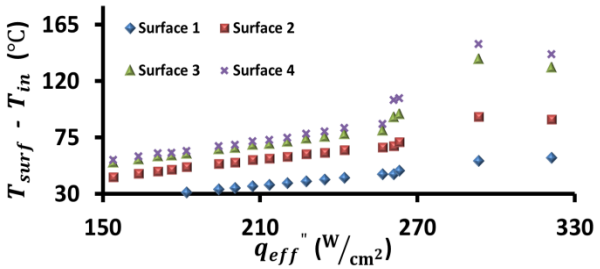

Figure 9: Surface Temperature-Heat Flux Experimental Data

A heat loss experiment was done by evacuating the loop and vacuuming the entire system using vacuum pump. All the heaters were then powered on and the heater temperatures were monitored. For a range of heater temperatures between 25-130 ℃, the power dissipated was calculated based on the applied voltage and current to the chip. Figure 10 shows the temperature of each heater recorded in the heat loss experiment. The maximum heat loss of 4.9 W occurred at 130 ℃, which was only 2.6% of the heat flux applied to the chip, under flow conditions. The maximum mass flux of 1,610 kg/m^{2}s was calculated for the heat flux of 326 W/cm^2.

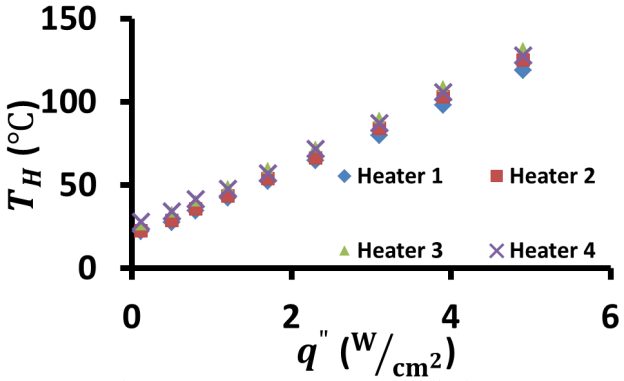

Figure 10: Heaters Temperature Distributions Versus Heat Loss Values

Table 3 summarizes the uncertainties of each parameter within experiment measurements.

Table 3: Uncertainty of Parameters

Quantity	±Uncertainty
Current (A)	0.5%
Voltage (V)	0.05%
Heater Power (W)	0.55%
Temperature (℃)	0.5 ℃
Pressure (kPa)	0.25%

CONCLUSIONS

Two phase flow of refrigerant R245fa in a microgap with staggered hydrofoil pin fins was studied for a range of heat fluxes from 151 W/cm^2 to 326 W/cm^2. The results are expressed as exit vapor quality, and surface temperature. The flow in the microgap was visualized using a high speed video camera. A maximum quality of about 13% was calculated at the outlet of the test section for the maximum heat flux of 326 W/cm^2. The visualization showed a new flow feature in the region in the microgap starting at 264 W/cm^2. The new regime had covered part of the gap with only vapor and this region became expanded as heat flux increased.

ACKNOWLDEGMENTS

The authors thank the DARPA IceCool Fundamentals Program for providing the financial support for this research.

REFERENCES

[1] A. Bar-Cohen, J. R. Sheehan, and E. Rahim, "Two-Phase Thermal Transport in Microgap Channels-Theory, Experimental Results, and Predictive Relations" Microgravity Science and Technology, vol. 24, pp. 1-15, 2012.

[2] T. Alam, P. S. Lee, C. R. Yap, and L. Jin, "Experimental investigation of local flow boiling heat transfer and pressure drop characteristics in microgap channel" International Journal of Multiphase Flow, vol. 42, pp. 164-174, 2012.

[3] J. Lee and I. Mudawar, "Two-phase flow in high-heat-flux micro-channel heat sink for refrigeration cooling applications: Part I - pressure drop characteristics" International Journal of Heat and Mass Transfer, vol. 48, pp. 928-940, 2005.

[4] Daxiang Deng, Wei Wan, Yong Tang, Zhenping Wan, and Dejie Liang, "Experimental investigations on flow boiling performance of reentrant and rectangular microchannels – A comparative study" International Journal of Heat and Mass Transfer, vol. 82, pp. 435-446, 2015.

[5] W. L. Qu and I. Mudawar, "Measurement and prediction of pressure drop in two-phase micro-channel heat sinks" International Journal of Heat and Mass Transfer, vol. 46, pp. 2737-2753, 2003.

[6] A. Kosar and Y. Peles, "Convective flow of refrigerant (R-123) across a bank of micro pin fins" International Journal of Heat and Mass Transfer, vol. 49, pp. 3142-3155, 2006.

[7] M. Law, P.S. Lee, "Comparative study of temperature and pressure instabilities during flow boiling in straight- and 10° oblique-finned microchannels", International Conference on Applied Energy, vol. 75, pp. 3105-3112, 2015.

[8] T.-W. Lim, S.-S. You, J.-H. Choi, and H.-S. Kim, "Experimental Investigation of Heat Transfer in Two-Phase Flow Boiling" Experimental Heat Transfer, vol. 28, pp. 23-36, 2015.

[9] W. Qu and I. Mudawar, "Flow boiling heat transfer in two-phase micro-channel heat sinks—I. Experimental investigation and assessment of correlation methods"

International Journal of Heat and Mass Transfer, vol. 46, pp. 2755-2771, 2003.

[10] S. Krishnamurthuy and Y. Peles, "Flow boiling of water in a circular staggered micro-pin fin heat sink" International Journal of Heat and Mass Transfer, vol. 51, pp. 1349-1364, 2008.

[11] W. Qu and I. Mudawar, "Measurement and correlation of critical heat flux in two-phase micro-channel heat sinks" International Journal of Heat and Mass Transfer, vol. 47, pp. 2045-2059, 2004.

[12] S. Lee, I. Mudawar, "Investigation of flow boiling in large micro-channel heat exchangers in a refrigeration loop for space applications" International Journal of Heat and Mass Transfer, vol. 97, pp. 110-129, 2016.

[13] A. Kosar and Y. Peles, "Boiling Heat Transfer in a Hydrofoil-Based Micro Pin Fin Heat Sink" International Journal of Heat and Mass Transfer, vol. 50, pp. 1018-1034, 2007.